Highlights from the LHCb experiment

Saverio Mariani[1,*], on behalf of the LHCb collaboration

[1]European Organization for Nuclear Research (CERN), Geneva, Switzerland

Abstract. LHCb has a complete and more and more attractive nuclear physics programme, covering the analysis of the ion data collected at the LHC and leveraging on the unique possibility to operate in fixed-target mode by injecting gas in LHC with the System for Measuring Overlap with Gas. In this document, recent results in small and large systems presented at the 2024 edition of the International Conference on Hard and Electromagnetic Probes of High-Energy Nuclear Collisions (Hard Probes 2024, HP2024) are discussed.

1 LHCb as a heavy-ion and fixed-target experiment

The LHCb experiment at CERN is a single-arm spectrometer [1, 2] instrumenting the pseudorapidity range $\eta \in [2, 5]$, not accessible with full instrumentation by the other LHC detectors. It includes a tracking system, which provides a measurement of the momentum, p, of charged particles with a relative uncertainty that varies from 05% at low momentum to 1.0% at 200 GeV. It is composed of a silicon-strip vertex detector surrounding the proton-proton, pp, interaction region and tracking stations upstream and downstream of a dipole magnet. Different types of particles are distinguished by combining the information of several subdetectors, namely two ring-imaging Cherenkov detectors, a calorimetric and a muon system. Since 2011, LHCb is also equipped with a System for Measuring Overlap with Gas (SMOG [3]), capable of injecting gas in the LHC beam-pipe to allow a measurement of the LHC beams transverse profiles through the imaging of the reconstructed beam-gas collisions. With a forward, fixed-target-like, geometry of its detector and the availability of a gaseous target, LHCb is currently the only LHC detector capable of operating in both collider and fixed-target mode. A summary of the collected datasets in the so-called LHC Run2, between 2015 and 2018, is shown in left Fig. 1. Injections of helium, neon and argon have been performed with either the protons or the lead ions circulating in LHC, allowing to probe increasing system-size collisions. Unfortunately, the luminosity was limited as these data were mostly collected in dedicated and short periods, and the injected gas pressure could not be raised above $\mathcal{O}(10^{-7})$ mbar. In collider mode, LHCb collected in Run2 pp collisions corrisponding to an integrated luminosity of about $6\,\text{fb}^{-1}$, enabling several world-record precision measurements. LHCb also joined the ion data-taking campaigns, with the datasets in proton-lead, pPb, or lead-lead, PbPb, shown in right Fig. 1. While smaller systems were always acquired with excellent LHCb performance, saturation of the tracking system was such that only peripheral PbPb collisions up to about 60% centrality could be acquired and analysed.

*e-mail: saverio.mariani@cern.ch

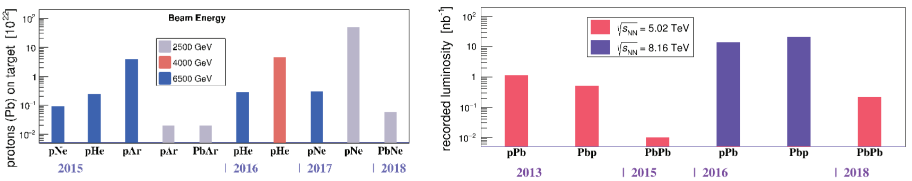

Figure 1. Summary of the LHCb collected datasets in (left) fixed-target and (right) ion collider mode. Different colours are used for different beam or nucleon-nucleon centre-of-mass energies, and (left) particles on targets or (right) luminosities are also indicated.

Between 2018 and 2022, LHCb faced a major upgrade [4], mainly consisting of the replacement of the full tracking system to cope with a factor-five-increased pp instantaneous luminosity and to improve the achievable spatial granularity. The hardware trigger stage, reducing in Run2 the rate from about 40 MHz collision rate to 1 MHz, was also dropped and the detectors read-out electronics replaced. The detector is now being completely read-out, aligned and processed in real-time with a software-only application. The SMOG system also was upgraded as SMOG2 [5, 6]. While the gas was injected in Run2 in the whole box containing the innermost tracking detector, the VELO, SMOG2 is a 20-cm-long storage cell with a 1 cm diameter in its closed position. As the gas injection happens in the middle of the cell, the gas areal density seen from the beam, and as a consequence the beam-gas instantaneous luminosity, can increase by up to two orders of magnitude with respect to the previous system. Moreover, as the SMOG2 cell is installed about 40 cm upstream of the pp interaction region, and interesting events are selected on the basis of reconstructed tracks, a continuous beam-beam and beam-gas data-taking has been proven in 2022 [6, 7]. In 2024, LHCb hence operated with two simultaneous interaction points, collecting collisions of two different systems and at two different centre-of-mass energies. The resulting collected samples, shown in left Fig. 2, exceed that of Run2 by up to three orders of magnitude and include, for the first time, also non-noble gases like hydrogen and deuterium. The tracking system upgrade also clearly benefit the ion programme, allowing semi-central PbPb collisions to be efficiently reconstructed. As demonstrated in 2023 by e.g. right Fig. 2 [8] for the $K_s \to \pi^+\pi^-$ decay, signal peaks down to 30% centrality are identified. In 2024, leveraging on the inversion of the LHCb magnet polarity and on optimisations of the beam settings, a larger instantaneous luminosity by a factor $\sim$ 70% was achieved and the collected PbPb sample, corresponding to 0.43 nb^{-1}, is now the largest one available.

A further upgrade of the experiment, LHCb Upgrade II [9], is being conceived to start operating in 2036. The detectors will be required to cope with a pp instantaneous luminosity larger than 10^{34} cm^{-2}s^{-1}, and will mostly be equipped with timing to discriminate among the $\mathcal{O}(40)$ simultaneous pp collisions. The increased spatial and timing capabilities will largely benefit ion data acquisition, and by design reconstruction of the full PbPb centrality is supported. Also, the addition of tracking station in the magnet will widen the detector acceptance by allowing the reconstruction of particles down to $p_{\mathrm{T}} \sim 50$ MeV. The related unique prospects are discussed in Ref. [10]. An upgrade of the fixed-target system, called LHCSpin [11], is also being planned. This targets a gas storage cell similar to SMOG2, but where the injected

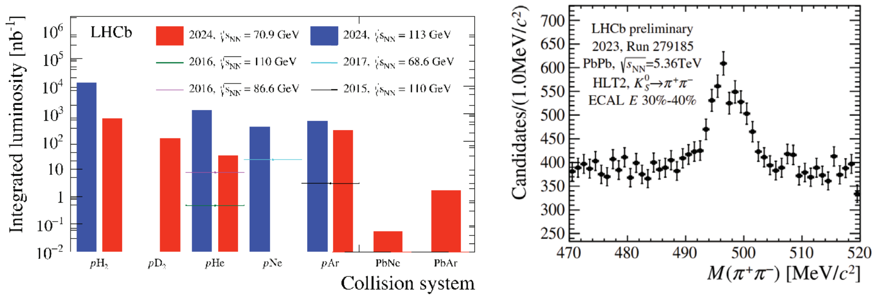

Figure 2. (Left) Summary of the samples collected with SMOG2 in 2024 by injecting hydrogen, deuterium, helium, neon and argon with both proton and lead ions circulating in LHC. When compared to some of the samples illustrated in Fig. 1, larger luminosities by up to three orders of magnitude are found. (Right) Invariant mass distribution for $K_s \to \pi^+\pi^-$ candidates, reconstructed in PbPb collisions with 30 to 40% centrality.

gas can be polarised. A completely new field would hence be accessible at LHCb and at LHC.

2 Studies of strange and charm hadrons

With the large variety of datasets described in the previous section, several studies on strange and charm hadrons are being performed. As the the phenomena observed in large collision systems occur from the interplay between Quark and Gluon Plasma (QGP) and Cold Nuclear Matter effects, i.e. the modifications of the dynamics due to the nuclear environment, measurements in various collision systems and at different energies are required in order to disentangle them. In this respect, LHCb with SMOG is a unique facility, as the collision energy scale, $\sqrt{s_{\rm NN}} \in [27, 114]$ GeV for a beam energy between 450 GeV and 7 TeV, and the kinematic phase space, high-x at intermediate Q^2, are mostly unexplored by previous experiments.

Several cross-section measurements results had been published already by analysing SMOG data, such as for prompt antiprotons in $\sqrt{s_{\rm NN}} = 110$ GeV pHe collisions [12] and for J/ψ [13] and D^0 [14] in $\sqrt{s_{\rm NN}} = 68.5$ GeV pNe and PbNe [15] collisions. Recently, the measurement of the $\phi(1020) \to K^+K^-$ cross-section in the same pNe dataset, as shown in left Fig. 3, was added to this list [16]. The cross-section is measured double-differentially as a function of the transverse momentum and the rapidity, and results are generally found to be underestimated by recent theoretical models such as PYTHIA8 and EPOS4. The results therefore provide useful information to tune phenomenological models on strangeness production, as needed to constitute a key reference for QGP searches in heavier colliding systems. Other than production, also hadron polarisation is being investigated in SMOG fixed-target collisions. In a recent result [17], the transverse polarisations of Λ and $\bar{\Lambda}$ baryons was measured in $\sqrt{s_{\rm NN}} = 68.5$ GeV pNe collisions. The former is found to be consistent with previous measurements, in particular by the HERA-B; the latter with zero as expected.

Strangeness is also being studied at LHCb in collider mode, where heavier probes are accessible. In particular, by studying hadron yields as a function of the produced particle multiplicity, clear indications of final-state effects can be observed. Among these, while ratios among different charm or beauty hadrons in vacuum are purely

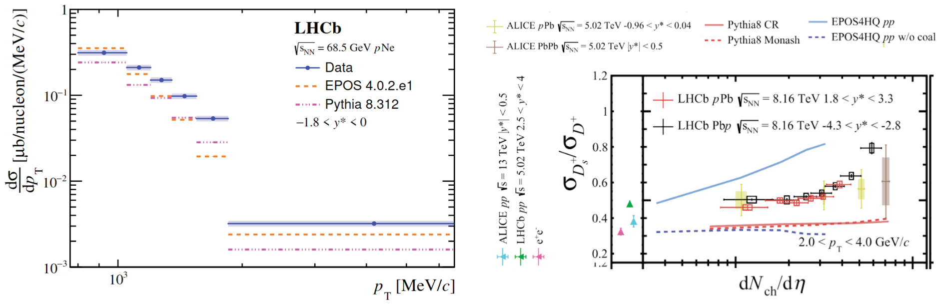

Figure 3. (Left) Differential cross-section as a function of the transverse momentum for $\phi(1020) \to K^+K^-$ production in $\sqrt{s_{\mathrm{NN}}} = 68.5$ GeV pNe collisions [16]. (Right) Ratio between the D_s^+ and D^+ mesons production as a function of the charged particle density in 8.16 TeV pPb collisions [18], compared to theoretical models and previous measurements from LHCb and ALICE collaborations.

determined by fragmentation, other effects, such as coalescence, are thought to be relevant at high multiplicities. In this direction, LHCb has first published the measurement of the B_s^0-to-B^0 ratio in pp collisions, showing indications of an increased trend with mupltiplicity. A recent similar result, but in the charm sector, has been published in pPb collisions [18], and is shown in right Fig. 3. While at low multiplicity the extrapolated ratio is consistent with the vacuum limit, the results confirm also in this system the increasing trend, not reproduced by current theoretical models.

3 Quarkonia and exotica from small to large systems

Heavy quarkonia, bound states of heavy quark-antiquark pairs, are golden probes to study Quantum ChromoDynamics (QCD). As these states are created at the early stages of the collision, quarkonia experience in large systems the QGP formation and evolution. The experimentally observed quarkonia yields hence result from the interplay of different effects: quarkonia melting due to dissociation in the QGP or due to interactions with comoving particles, quarkonia regeneration due to the high quark-antiquark density and so on. In order to isolate medium-induced effects, quarkonia yields are typically measured in nuclear collisions relatively to pp. Several results, mostly for charmonia states, have already been published by LHCb in pp and pPb collisions. Recently, these studies have been extended to bottomonia states in pp collisions [19] and to the PbPb collision system [20], with examples of the results shown in Fig. 4. On the left, the $\Upsilon(2S)$-to-$\Upsilon(1S)$ cross-section ratio in $\sqrt{s} = 13$ TeV pp collisions is shown as a function of the transverse momentum. When compared to previous results from the CMS and LHCb experiments, the achieved precision is much improved. A similar trend is observed considering the $\Upsilon(3S)$-to-$\Upsilon(1S)$ ratio and the ratios measured as a function of the charged particle multiplicity are found to be consistent with the description of the comover model [21].

Right Fig. 4 shows the $\psi(2S)$-to-J/ψ cross-section ratio in $\sqrt{s_{\mathrm{NN}}} = 5.02$ TeV PbPb collisions as a function of the number of participants. Following the saturation of the Run2 detector tracking system, only semi-peripheral PbPb collisions up to about 60% centrality are studied. The obtained result is found to be flat and consistent with previous results from other experiments, albeit with larger uncertainties. The

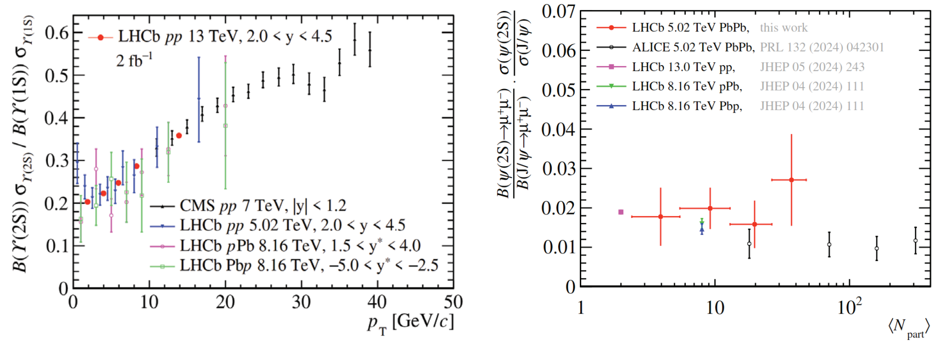

Figure 4. (Left) Measurement of the $\Upsilon(2S)$-to-$\Upsilon(1S)$ cross-section ratio in $\sqrt{s} = 13$ TeV pp collisions as a function of the transverse momentum [19], compared to previous CMS and LHCb results. (Right) Measurement of the $\psi(2S)$-to-J/ψ ratio in $\sqrt{s} = 5.02$ TeV PbPb collisions as a function of the number of participants [20], compared to previous ALICE and LHCb results.

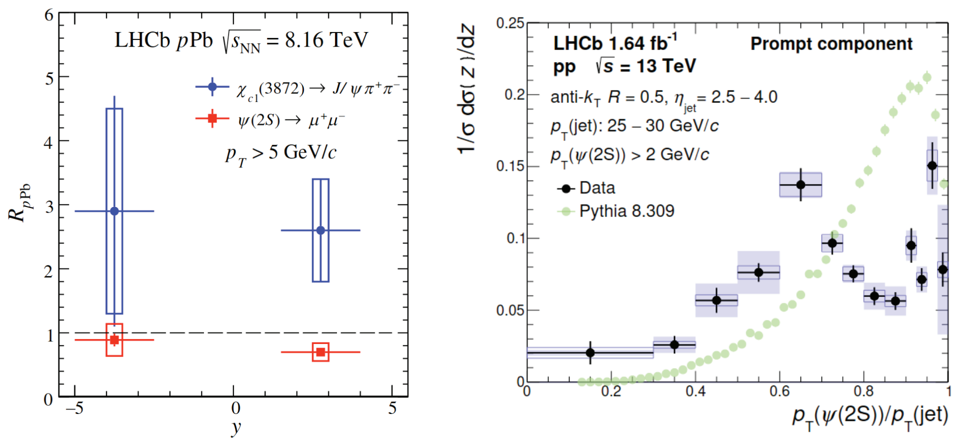

Figure 5. (Left) Nuclear modification factor for $\chi_c(3872) \to J/\psi\pi^+\pi^-$ decays as a function of rapidity [22], measured in $\sqrt{s_{\rm NN}} = 8.16$ TeV pPb collisions. (Right) Distribution of the $p_{\rm T}$ fraction for prompt $\psi(2S)$ [23] in jets, not reproduced by the PYTHIA model.

incoming Run3 data will allow to remarkably reduce those uncertainties, dominated by the statistical contribution, and to cover a larger fraction of the centrality range.

Other than quarkonia, LHCb has excellent capabilities in studying exotic probes as well. As these are composed of four or five quarks, they offer a complementary facility with respect to standard hadrons, given that the interplay among the suppression and regeneration effects might be different. Recently, LHCb released its first measurement for the $\chi_c(3872)$-to-$\psi(2S)$ ratio in pPb collisions [22]. Compared with an LHCb measurement for the same quantity in pp collisions and with one by CMS in PbPb, an increasing trend of the ratio with the system size is found. As such a result has some intrinsic ambiguity, due to the two possibilities of an enhancement of the $\chi_c(3872)$ or a suppression of the $\psi(2S)$, the $\chi_c(3872)$ nuclear modification is also measured for the

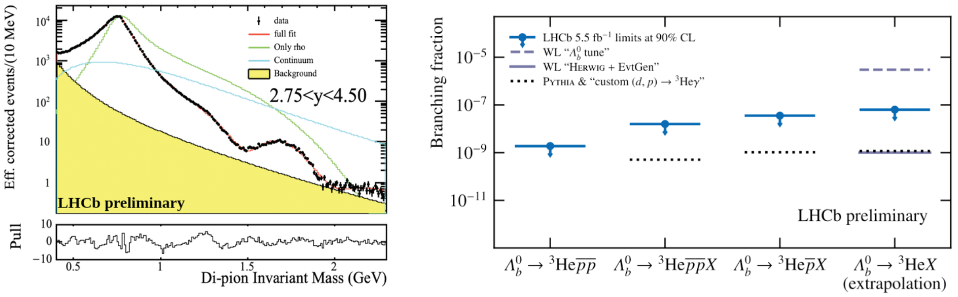

Figure 6. (Left) Invariant mass distribution for opposite-sign pions produced in Ultra-Peripheral $\sqrt{s_{\mathrm{NN}}} = 5.02$ TeV PbPb collisions [24]. The invariant mass distribution is modelled with a parametric function (in red), obtained from the sum of resonant and non-resonant components in the complex phase-space. (Right) Best limits on the branching fractions of several Λ_b decays in final-states with helium [25].

first time and shown in left Fig. 5. Albeit affected by large uncertainties, a positive value is found, confirming a $\chi_c(3872)$ enhancement and a potential dominance of coalescence over breakup.

A second recent result studies the same probes, $\chi_c(3872)$ and $\psi(2S)$, but reconstructed in *pp* collisions within jets. Leveraging on the larger available statistics, the prompt and from-b decays contributions can be studied separately with high precision. While the former case is found to be correctly reproduced by PYTHIA, a two-peaks structure found for the $\psi(2S)$, especially at low transverse momentum as shown for example in right Fig. 5, demands new theoretical developments.

4 More possibilities at LHCb

Simultaneously to hadronic PbPb collisions, ion data-taking at LHCb allows rich samples of Ultra-Peripheral Collisions, where interactions are mediated via photons or other colourless objects, to be collected. As these events are characterised by a very-low multiplicity in the detector, namely the final-state particles only, they are always reconstructed with very high efficiency and allow to probe the low-x initial state of the colliding nuclei. A measurement for the production of ρ mesons has recently been released by analysing 2018 PbPb data. Left Fig. 6 shows the invariant mass distribution for opposite-sign pions produced in these collisions, which extended up to about 2.5 GeV. With such a high-statistics sample, past parametrisations for the $\rho - \omega$ resonances interference could be tested up to high masses, where they were found to fail. A new parametrisation, shown in red in the figure, has instead been successfully proposed. This includes a second resonance around 1.8 GeV, consistent with the PDG ρ', previously observed by ALICE and STAR and now unambiguously confirmed by these new data. Cross-sections for all these states and their p_{T} spectrum, providing further insights into the interference pattern, are also being measured.

Despite not initially foreseen at LHCb, new techniques for nuclei identification have been developed. For the case of helium, these rely on the nucleus energy loss in the LHCb detector and have been found [26] to provide in the Run2 *pp* collision data an almost background-free sample of more than 10^5 (anti)helium nuclei. Such a high-statistics sample enables to investigate different mechanisms for helium production and, in particular, a possible decay of the $\bar{\Lambda}_b$ baryon into final-states including helium. Following the hints for observation of anti-helium particles in cosmic rays by the AMS experiment [27], in excess with respect to the expectations, such process has been proposed [28] as a feasible explanation, alternative to a possible dark matter decay or annihilation. To fully explain AMS observations, a minimum 10^{-6} branching ratio for the $\bar{\Lambda}_b \to \overline{\mathrm{He}}$ is needed. Right Fig. 6 shows LHCb results for the fully reconstructed $\Lambda_b \to \mathrm{He}\bar{p}\bar{p}$ decay and the extrapolated ones for more inclusive modes. The obtained limit is found to be below the required one by more than one order of magnitude, excluding such a process as an explanation for the AMS claims.

5 Conclusions

In conclusion, LHCb has a wider and wider nuclear physics programme, covering soft and hard probes from small to large systems. Additionally to the LHC heavy-ion data-takings, LHCb also can rely on the unique opportunities offered by the fixed-target system, probing an energy and kinematic phase space mostly unexplored so far. In this contribution, a few recent examples of this programme are discussed, showing how in most cases the achieved precision dominates the worldwide state of the art.

References

[1] A.A. Alves Jr. et al. (LHCb collaboration), The LHCb detector at the LHC, JINST **3**, S08005 (2008). 10.1088/1748-0221/3/08/S08005
[2] R. Aaij et al. (LHCb collaboration), LHCb detector performance, Int. J. Mod. Phys. **A30**, 1530022 (2015), 1412.6352. 10.1142/S0217751X15300227
[3] M. Ferro-Luzzi, Proposal for an absolute luminosity determination in colliding beam experiments using vertex detection of beam-gas interactions, Nucl. Instrum. Meth. **A553**, 388 (2005). 10.1016/j.nima.2005.07.010
[4] R. Aaij et al. (LHCb collaboration), The LHCb Upgrade I, JINST **19**, P05065 (2024), 2305.10515. 10.1088/1748-0221/19/05/P05065
[5] R. Aaij et al. (LHCb collaboration), LHCb SMOG Upgrade (2019), CERN-LHCC-2019-005.
[6] O. Boente Garcia et al., High-density gas target at the LHCb experiment, Phys. Rev. Accel. Beams **27**, 111001 (2024), 2407.14200. 10.1103/PhysRevAccelBeams.27.111001
[7] S. Mariani, Fixed-target physics with the LHCb experiment at CERN (2021), CERN-THESIS-2021-3131.
[8] First invariant mass spectra and performance figures of the 2023 ion run (2023), LHCb-FIGURE-2023-030.
[9] R. Aaij et al. (LHCb collaboration), LHCb Framework TDR for the LHCb Upgrade II Opportunities in flavour physics, and beyond, in the HL-LHC era (2022), CERN-LHCC-2021-012.
[10] R. Aaij et al. (LHCb collaboration), Opportunities for heavy-ion and fixed-target physics with LHCb Upgrade II (2025), LHCb-PUB-2024-007.
[11] C.A. Aidala, A. Bacchetta, M. Boglione, G. Bozzi, V. Carassiti, M. Chiosso, R. Cimino, G. Ciullo, M. Contalbrigo, U. D'Alesio et al., The LHCSpin project (2019), 1901.08002.

[12] R. Aaij et al. (LHCb collaboration), Measurement of antiproton production in pHe collisions at $\sqrt{s_{NN}}$ = 110 GeV, Phys. Rev. Lett. **121**, 222001 (2018), 1808.06127. 10.1103/PhysRevLett.121.222001

[13] R. Aaij et al. (LHCb collaboration), Charmonium production in pNe collisions at $\sqrt{s_{\rm NN}}$ = 68.5 GeV , Eur. Phys. J. **C83**, 625 (2023), 2211.11645. 10.1140/epjc/s10052-023-11608-6

[14] R. Aaij et al. (LHCb collaboration), Open charm production and asymmetry in pNe collisions at $\sqrt{s_{\rm NN}}$ = 68.5 GeV, Eur. Phys. J. **C83**, 541 (2023), 2211.11633. 10.1140/epjc/s10052-023-11641-5

[15] R. Aaij et al. (LHCb collaboration), J/ψ and D^0 production in $\sqrt{s_{\rm NN}}$ = 68.5 GeV PbNe collisions, Eur. Phys. J. **C83**, 658 (2023), 2211.11652. 10.1140/epjc/s10052-023-11674-w

[16] R. Aaij et al. (LHCb collaboration), Measurement of ϕ meson production in fixed-target pNe collisions at $\sqrt{s_{NN}}$ = 68.5 GeV at LHCb (2024), Submitted to JHEP, 2411.09343.

[17] R. Aaij et al. (LHCb collaboration), Transverse polarisation measurement of Λ hyperons in pNe collisions at $\sqrt{s_{NN}}$=68.4 GeV with the LHCb detector, JHEP **09**, 082 (2024), 2405.11324. 10.1007/JHEP09(2024)082

[18] R. Aaij et al. (LHCb collaboration), Observation of strangeness enhancement with charm mesons in high-multiplicity pPb collisions at $\sqrt{s_{NN}}$ = 8.16 TeV, Phys. Rev. **D110**, L031105 (2024), 2311.08490. 10.1103/PhysRevD.110.L031105

[19] R. Aaij et al. (LHCb collaboration), Measurement of the multiplicity dependence of Υ production ratios in pp collisions at $\sqrt{s}$ = 13 TeV (2025), Submitted to JHEP, 2501.12611.

[20] R. Aaij et al. (LHCb collaboration), Measurement of $\psi(2S)$ to J/ψ cross-section ratio as a function of centrality in PbPb collisions at $\sqrt{s_{NN}}$ =5.02 TeV (2024), Submitted to JHEP, 2411.05669.

[21] E. Ferreiro, Charmonium dissociation and recombination at LHC: Revisiting comovers, Physics Letters B **731**, 57–63 (2014). 10.1016/j.physletb.2014.02.011

[22] R. Aaij et al. (LHCb collaboration), Modification of $\chi_{c1}(3872)$ and ψ(2S) production in pPb collisions at $\sqrt{s_{NN}}$ = 8.16 TeV, Phys. Rev. Lett. **132**, 242301 (2024), 2402.14975. 10.1103/PhysRevLett.132.242301

[23] R. Aaij et al. (LHCb collaboration), Measurements of $\psi(2S)$ and $\chi_{c1}(3872)$ within fully reconstructed jets (2024), Submitted to Eur. Phys. J. C, 2410.18018.

[24] R. Aaij et al. (LHCb collaboration), A measurement of the differential cross-section for ρ mesons produced in ultra-peripheral PbPb collisions (2024), in preparation, to be submitted to JHEP.

[25] R. Aaij et al. (LHCb collaboration), Antihelium production in $\overline{\Lambda_b}$ decays (2024), LHCb-CONF-2024-005.

[26] R. Aaij et al. (LHCb collaboration), Helium identification with LHCb, JINST **19**, P02010 (2024), 2310.05864. 10.1088/1748-0221/19/02/P02010

[27] S. Ting, Latest results from AMS on the International Space Station (8 June 2023), https://indico.cern.ch/event/1275785/

[28] M.W. Winkler, T. Linden, Dark Matter Annihilation Can Produce a Detectable Antihelium Flux through $\bar{\Lambda}_b$ Decays, Phys. Rev. Lett. **126**, 101101 (2021), 2006.16251. 10.1103/PhysRevLett.126.101101